New Journal of Physics
The open-access journal for physics

Theoretical and experimental investigations of three-terminal carbon nanotube relays

S Axelsson[1,4], E E B Campbell[2,5], L M Jonsson[1], J Kinaret[1], S W Lee[2,3], Y W Park[3] and M Sveningsson[2]

[1] Department of Applied Physics, Chalmers University of Technology, SE-412956 Göteborg, Sweden
[2] Department of Physics, Göteborg University, SE-41296 Göteborg, Sweden
[3] School of Physics and Nano Systems Institute-National Core Research Center, Seoul National University, Seoul 151-747, Korea
E-mail: Eleanor.Campbell@fy.chalmers.se

New Journal of Physics **7** (2005) 245
Received 2 August 2005
Published 29 November 2005
Online at http://www.njp.org/
doi:10.1088/1367-2630/7/1/245

Abstract. We present theoretical and experimental investigations of three-terminal nanoelectromechanical relays based on suspended carbon nanotubes. A charge is induced in the nanotube by applying a voltage to an underlying gate electrode thus inducing the nanotube to bend and make contact with a drain electrode. Such devices have potential applications as fast switches, logic devices, memory elements and pulse generators. We describe two modes of operation: a contact mode where the nanotube makes physical contact with the drain electrode and a non-contact mode where electrical contact between the nanotube and the drain electrode is made via a field emission current.

[4] Present address: Siemens Industrial Turbomachinery AB, SE-61283 Finspong, Sweden.
[5] Author to whom any correspondence should be addressed.

PII: S1367-2630(05)04903-7

Contents

1. Introduction

Carbon nanotubes have extraordinary properties that make them ideal building blocks for nanoelectromechanical devices (NEMS). They are light, have high Young's moduli and can be elastically deformed without breaking (e.g. Dresselhaus *et al* 2001). In addition, multiwalled nanotubes typically behave as metals and can carry very high currents (Collins *et al* 2001).

The nanorelay is a nanoelectromechanical component in which a conducting carbon nanotube is electrostatically bent to close an electric circuit. The three-terminal structure, in which the voltage applied to bend the nanotube is disconnected from the source–drain voltage, was introduced by Kinaret *et al* (2003) and has subsequently been studied experimentally (Lee *et al* 2004a) and theoretically (Jonsson *et al* 2004a, b, Hwang and Kang 2005). The nanotube bends as a response to an electrostatic force, which is always present between the plates of a charged capacitor. The force is a result of Coulomb attraction between the polarization charges on the capacitor plates. Related two-terminal switches have also been considered (Desquesnes *et al* 2002, Ke and Espinosa 2003). The relay structure requires fabricating a nanotube supported at one end via contact to a source electrode and freely suspended over a gate and drain electrode. For practical reasons, this requires multiwalled nanotubes since single-walled nanotubes lack the required rigidity to form the suspended structure. Multiwalled nanotubes have the additional advantage of being able to transport significantly more current than single-walled nanotubes.

The nanotube nanorelay has a wide range of possible potential applications. Some that have been discussed include logic devices, memory elements, pulse generators and current or voltage amplifiers (Kinaret *et al* 2003, Jonsson *et al* 2004a). Some more potentially interesting applications involve the high-frequency properties of the devices. Theoretical studies (Jonsson *et al* 2004b) have predicted that the relay will show a nonlinear electromechanical resonant behaviour for frequencies in the GHz regime. The resonant frequencies depend on the gate-bias voltage, which can be exploited to tune the resonance to a desired frequency.

The three-terminal nanorelay has been predicted to operate in two different regimes known as the contact mode and the non-contact mode (Jonsson *et al* 2004b). Each of these operating modes has specific characteristics. The movies that can be linked to from figure 1 illustrate the

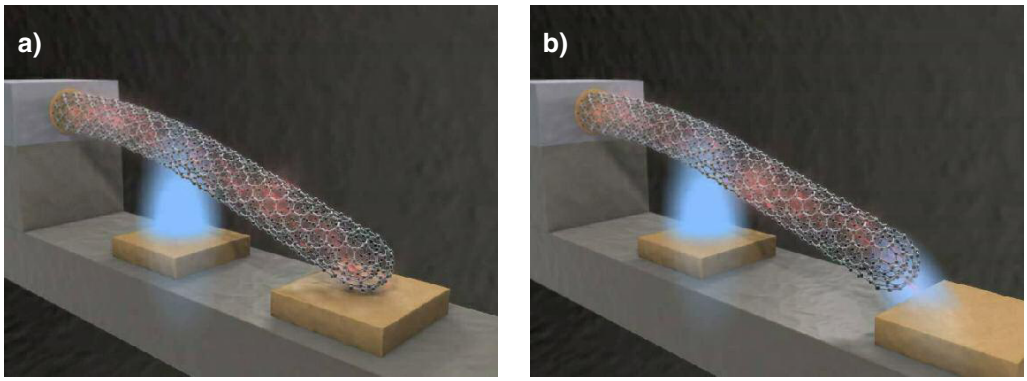

Figure 1. Frames from movies illustrating the operating characteristics of the nanotube relay in (a) the contact mode and (b) the non-contact mode. A voltage applied to the central gate electrode (schematically indicated by the blue colouring) induces the nanotube to bend until electrical contact is made with the drain electrode. The movies can be seen by clicking on the links: contact and non-contact.

two different modes. In the contact mode, figure 1(a), the nanotube is deflected until it touches the drain electrode. This device is operated with a relatively small source–drain voltage (typically <1 V). The non-contact mode, figure 1(b), relies on electron field emission from the nanotube tip to make electrical contact with the drain electrode and needs to be operated at substantially higher source–drain voltages (greater than the nanotube work function).

In this paper, we will concentrate on the dc properties of the three-terminal nanorelay since so far there have been no experimental reports of the high-frequency behaviour. We describe the theoretical model, emphasising new results on the theoretical modelling of the non-contact mode configuration. We then provide details of the fabrication procedure and present experimental investigations of a range of nanorelay structures, in both contact and non-contact modes. We show that the idea of the three-terminal nanorelay can be realized experimentally. The contact mode behaviour is quantitatively similar to the theoretical predictions, the main difference being due to the presence of adsorbates at the nanotube and electrode surfaces that influences the switching behaviour of the devices. Only preliminary experimental results are available for the non-contact mode but again the concept of the nanorelay also seems to work for this configuration. We discuss these first results and provide possible reasons for some discrepancy between the measurements and the theoretical predictions.

2. Theoretical model

A schematic illustration of the theoretical model for the nanorelay is shown in figure 2, together with the corresponding equivalent circuit. A metallic nanotube of length L and diameter d_o is suspended from a terraced insulating substrate such that one end is free to move and the other end is ohmically connected to a source electrode with an impedance Z. In FEMLAB, the nanotube is regarded as a thin perfectly conducting wire with circular cross-section and capped with a hemisphere. Two additional electrodes (gate and drain) are placed underneath the free end of

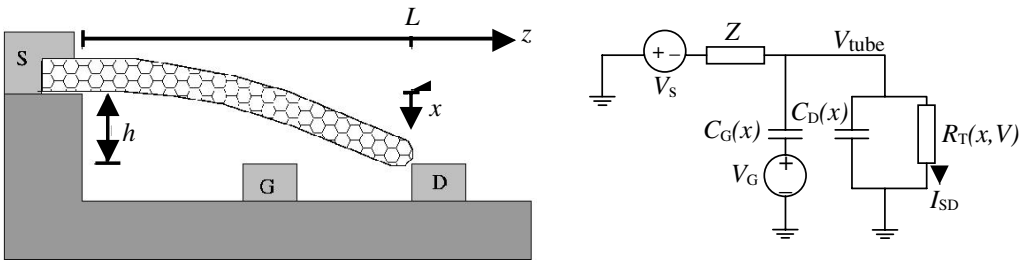

Figure 2. Schematic diagram of the nanotube relay together with the equivalent circuit diagram. One end of a conducting multiwall nanotube of length L, diameter d_o is attached to a source electrode (S) placed at a height h above a gate (G) and drain (D) electrode. The other end of the nanotube is free to move. The displacement x of the nanotube is measured towards the substrate. The gate electrode (G) is used to control the motion of the tip. The impedance Z is ohmic and describes the source–nanotube coupling. The nanotube–gate coupling is purely capacitive with the capacitance C_G, whereas the nanotube–drain coupling is a tunnel junction with tunnelling resistance $R_T(x)$ and capacitance $C_D(x)$. $V_{S,G,D}$ are the electrostatic potentials on the electrodes, in this example the drain electrode is grounded.

the nanotube. The vertical distance between the electrodes and the undeflected nanotube is h. The axis along the nanotube is labelled z. The drain electrode is placed at $z_D(\approx L)$ and the gate electrode at $z_G(< L)$. The nanotube–gate coupling is capacitive with capacitance $C_G\ (x)$, where x is the deflection of the nanotube from the horizontal position, and the nanotube–drain coupling is a tunnel junction with capacitance $C_D\ (x)$ and tunnelling resistance $R_T\ (x, V)$. The potential difference V between the source and gate and/or drain electrodes induces an excess charge q on the nanotube. Consequently, a capacitive force acts to deflect the nanotube tip in the vertical direction (x). If $z_D \leqslant L$, the nanotube tip makes mechanical contact with the drain electrode when the deflection is large enough $(x = h)$, thereby closing an electric circuit. This is referred to as the 'contact mode' (figure 1(a)). If, however, the nanotube is shorter than z_D by more than the tunnelling length $\lambda(\sim 0.5\ \text{Å})$, then the nanotube and the electrode never make physical contact. This is referred to as the 'non-contact mode' of operation (figure 1(b)).

The details of the theoretical model, in which the classical continuum elasticity theory is used to model the tube motion and the tunnelling rate is calculated using the Coulomb-blockade theory in the presence of an electromagnetic environment, have been given previously (Kinaret *et al* 2003, Jonsson *et al* 2004a) with emphasis on the contact mode of operation. Basically, the electrostatic and interatomic (van der Waals and short-range attraction) forces serve to deflect the carbon nanotube and provide an attractive interaction with the drain electrode. These forces are counterbalanced by the elastic forces that attempt to restore the nanotube to its original position. For a given applied gate voltage, the equilibrium position of the nanotube will be defined by the balance of the elastic, electrostatic and interatomic forces. Below, we will briefly review the predictions of the operation in the contact mode and then provide some new results on the modelling of the non-contact mode.

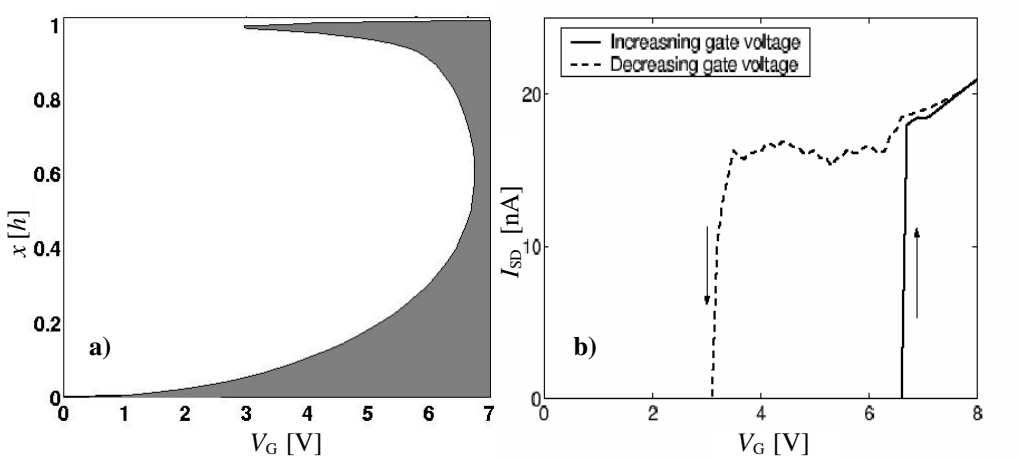

Figure 3. (a) Stability diagram for a nanorelay operating in the contact mode, calculated with the parameters given in the text. The shaded region indicates a net positive force pulling the nanotube onto the drain electrode. The unshaded region indicates a net negative force. The presence of more than one local equilibrium (no net force acting on the nanotube, shown by the dividing line between non-shaded and shaded regions) indicates hysteretic behaviour. (b) Calculated I_{SD}–V_G behaviour for the same nanotube with a source–drain potential of 10 mV. Adapted from Jonsson *et al* (2004a).

2.1. Contact mode

In this original relay design (Kinaret *et al* 2003), the electric circuit is closed when the nanotube tip establishes mechanical contact with the drain electrode. It was found that the magnitude of the van der Waals and short-range forces in the system are comparable to those of the elastic and electrostatic forces when the nanotube approaches the drain electrode (Kinaret *et al* 2003, Jonsson *et al* 2004a). This is in contrast to microelectromechanical switches where the interatomic forces can be neglected. This has major consequences for the operation of the nanorelay. The most important consequence is that the attractive force between the nanotube and the drain electrode can produce substantial hysteresis in the dependence of the source–drain current on the gate voltage. This can be advantageous for developing memory elements based on the relay (Jonsson *et al* 2004a), but can also lead to sticking ('stiction' problem) where it is not possible to remove the nanotube from the drain electrode. The problem may be alleviated by using shorter or stiffer nanotubes but this has the disadvantage of requiring a larger gate voltage for deflection (the 'pull-in' voltage). Alternatively, one could increase the contact resistance by coating the drain electrode with a thin insulating layer.

The details of the predicted operating characteristics depend very much on the parameters used for modelling the van der Waals and short-range forces (Jonsson *et al* 2004a). An example of the operation of a device where the surface forces are sufficiently low to release the nanotube when the gate voltage is turned off (Jonsson *et al* 2004a) is shown in figure 3. This has been calculated for the following set of parameters: $L = 120\,\text{nm}$, $d_o = 8.8\,\text{nm}$, $h = 5\,\text{nm}$, $z_D = L$, $z_G/z_D = 0.7$ and the Young's modulus of the nanotube=1 TPa. Figure 3(a) visualizes the effects of the surface forces in the form of a stability diagram. This shows the positions of zero net force

(local equilibria) on the nanotube as a function of gate voltage and deflection. The presence of more than one local equilibrium for a given gate voltage implies a hysteretic behaviour of the I_{SD}–V_G characteristics. The shaded region to the right of the curve corresponds to a net positive force, i.e. pulling the nanotube down to the drain electrode, whereas the region to the left of the curve corresponds to a net negative force, i.e. pulling the nanotube away from the drain electrode. The I_{SD}–V_G characteristics for the same device are shown in figure 3(b) for a source–drain potential of 10 mV. The 'pull-in' voltage for these parameters, i.e. where the nanotube snaps to the drain electrode, lies at 6.7 V, in good agreement with the stability diagram. The reverse transition occurs at a much lower gate voltage of approximately 3 V. A large hysteresis effect was also predicted from the results of MD simulations of a similar device (Hwang and Kang 2005).

2.2. *Non-contact mode*

Another approach to avoid the 'stiction' problem is to avoid physical contact between the nanotube and the drain electrode. In this case the electric circuit is closed by the field emission current induced from the tip of the nanotube (figure 1(b)). The nanotube–drain impedance varies exponentially with the nanotube–drain separation and may still be modified by using the gate voltage to bend the nanotube. However, the nanotube–drain impedance remains quite high even at the point of closest approach and operating the nanorelay in this non-contact mode requires higher source–drain voltages (greater that the nanotube work function).

Electron field emission is a tunnelling phenomenon. In general, tunnelling of individual electrons in a circuit involves excitation of collective modes in the electric environment. These phenomena have been extensively studied in connection with single-electron tunnelling, and are typically accounted for using the so-called $P(E)$ theory, which is reviewed e.g. by Ingold and Nazarov (1992). This theory considers the probability of the tunnelling electron giving energy E to the collective modes, which can be derived using the tunnelling-Hamiltonian approach and depends on the impedance of the electromagnetic environment of the tunnel junction. One of the assumptions underlying the customary tunnelling-Hamiltonian method is that the tunnelling matrix elements are taken to be only weakly dependent on the energy, which is valid provided that the energies involved are small compared to the Fermi energy and work function of the electrodes. This is usually the case in single-electron tunnelling in Coulomb-blockade structures, but the assumption is not justified in the field emission regime where the energy dependence of the tunnelling matrix elements is substantial.

No conclusive theoretical treatment exists in the limit where both the environment effects and energy-dependent tunnelling matrix elements are important. We have chosen to describe tunnelling in this regime as a two-step process, in which an electron with energy ε first tunnels through a barrier, and then excites environmental modes so that its final energy is ε–E. The elastic-tunnelling probability can be obtained by the Landauer–Büttiker theory by evaluating the energy-dependent transmission probability $T(E, V, x)$, where E is the energy of the tunnelling particle, V is the applied source–drain voltage and x is the tip–drain separation, resulting in the tunnelling rate (Axelsson 2004)

$$\Gamma(V, x) = \frac{2}{h} \int_{\max(0, E_F - eV)}^{E_F} \mathrm{d}E\, T(E, V, x) \int_0^{E - E_F + eV} \mathrm{d}E'\, P\left(E'\right), \tag{1}$$

where E_F is the Fermi level of the carbon nanotube. For large voltages, the second factor equals unity and the effect of the environmental modes is typically very small at the source–drain voltages

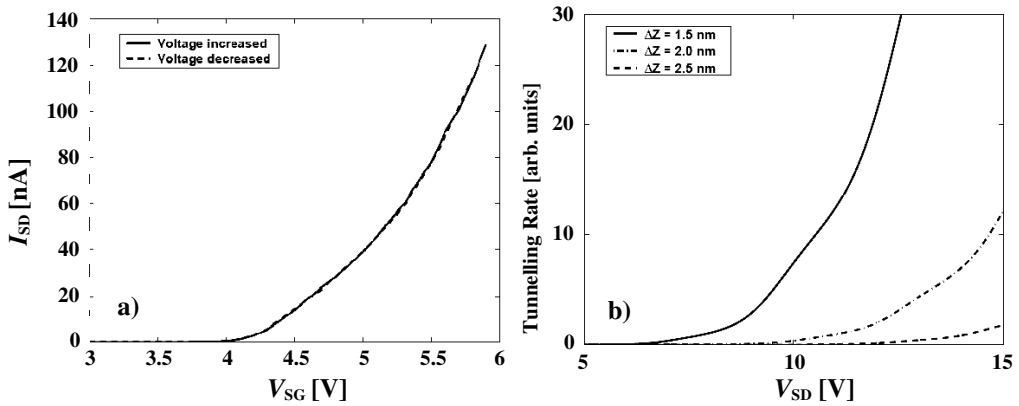

Figure 4. Modelled operating behaviour for a nanotube relay in the non-contact mode. (a) Dependence of the source–drain current on the gate voltage for a source–drain voltage of 11 V and 2 nm distance of closest approach. Note the absence of hysteresis. (b) Dependence of tunnelling rate on source–drain voltage for different distances of closest approach; full line, 1.5 nm; dot-dash line, 2 nm; dashed line, 2.5 nm.

for which an appreciable current flows in the non-contact mode structure. In a small (near-drain) non-contact mode device, the drain current, for a fixed source–drain voltage, increases rapidly as a function of the source–gate voltage. In figure 4(a), the modelling for a typical source–drain current at $V_{SD} = 11$ V is depicted for a nanotube with 5 nm diameter and 2 nm closest approach. The current for the gate voltage that corresponds to closest approach increases rapidly as a function of the source–drain voltage and depends sensitively on the minimum nanotube–drain separation as shown in figure 4(b). Note the absence of hysteresis in the I_{SD}–V_G characteristics for the non-contact mode of operation. The rough character of the calculated curves reflects current fluctuations due to the statistical nature of the transport.

In the non-contact mode, the local field at the nanotube tip determines the thickness of the tunnel barrier for applied voltages that exceed the nanotube work function. The local field depends on the device geometry and it is useful to consider separately two nanorelay structures: one in which the minimum nanotube–drain separation is comparable to the nanotube diameter (or less) and another in which the minimum separation greatly exceeds the nanotube diameter. We refer to these two cases as near-drain and far-drain structures. Most theoretical nanorelay studies thus far focus on the near-drain regime, whereas the experimental studies on non-contact mode relays (see below) have so far been in the far-drain limit.

2.2.1. Near-drain nanorelay. For two flat objects that are separated by a distance h that is much smaller than the transverse dimensions of the surfaces, the local field is simply the applied voltage divided by the separation between the objects. If the electrode dimensions are comparable or smaller than the electrode separation, the local fields at the electrodes may greatly exceed the average field. The ratio of the local field at the nanotube tip to the average field is known as the field enhancement factor β. For devices where the nanotube–drain separation is comparable with the nanotube diameter, β is nearly unity corresponding to no field enhancement. This is illustrated in figure 5(a). The absence of field enhancement in near-drain structures implies that

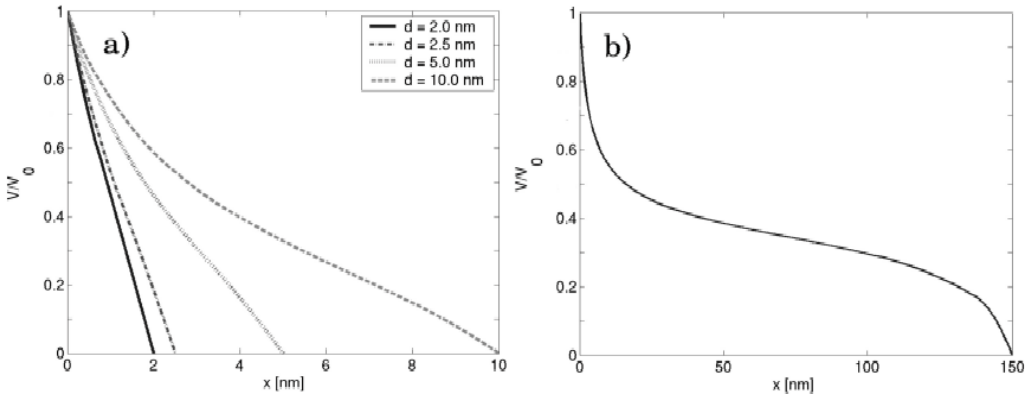

Figure 5. The ratio of the electrostatic potential to the applied voltage as a function of the distance from the nanotube tip to the drain electrode, x, illustrating the importance of field enhancement. The geometry is similar to that shown as an inset in figure 6. (a) Near-drain nanorelay where the nanotube–drain separation is comparable to the nanotube diameter, calculated for different nanotube diameters (2, 2.5, 5 and 10 nm). A linear plot indicates that the field enhancement factor is unity. (b) Far-drain nanorelay where the nanotube–drain separation is much larger than the nanotube diameter. Calculated for a nanotube diameter of 5 nm and a nanotube–drain separation of 150 nm. Note the sharp potential drop in the region close to the nanotube tip.

the I_D–V_{SD} characteristics are symmetric (assuming the same work functions for the nanotube and the drain).

2.2.2. Far-drain nanorelay. In the far-drain nanorelay, the field enhancement at the nanotube tip is substantial, as shown in figure 5(b) for a nanorelay with a 5 nm diameter nanotube 150 nm away from a strip-like drain electrode. Nearly 40% of the potential drop occurs within 7 nm from the nanotube, with an almost equal voltage drop near the drain electrode. The fields were calculated numerically using FEMLAB. The field enhancement factor increases with increasing nanotube–drain separation and with decreasing nanotube diameter. If we denote the nanotube diameter by d_o, the nanotube–drain separation by $\bar{h} = h - x$ and the drain dimension by b, the dimensionless field enhancement factor is given by a function $\beta(\bar{h}/d_o, b/d_0)$. For the case of a macroscopic anode (drain), the field enhancement factor at large nanotube–anode separation is known to vary linearly with the first argument, $\beta(\bar{h}/d_o, \infty)$ is approximately proportional to $\bar{h}/d_o$. This can be seen in experiments in which field emission from an individual carbon nanotube is studied in a combined STM/TEM apparatus, showing the same emission current for a given nanotube–anode distance at different applied voltages (Sveningsson *et al* 2005). Most of the voltage drop occurs near the nanotube tip, leading to an emission current that is independent of the nanotube–anode distance.

The drain current in a far-drain nanorelay depends sensitively on the width of the barrier through which electrons must tunnel. If the nanotube work function is φ and the local electric field is F, the barrier width is given by $W = \varphi/F = (\varphi/V_{SD})[\bar{h}/\beta(\bar{h}/d_o, b/d_o)]$, provided that the electric field is constant over the distance W. When the gate voltage is changed, the nanotube

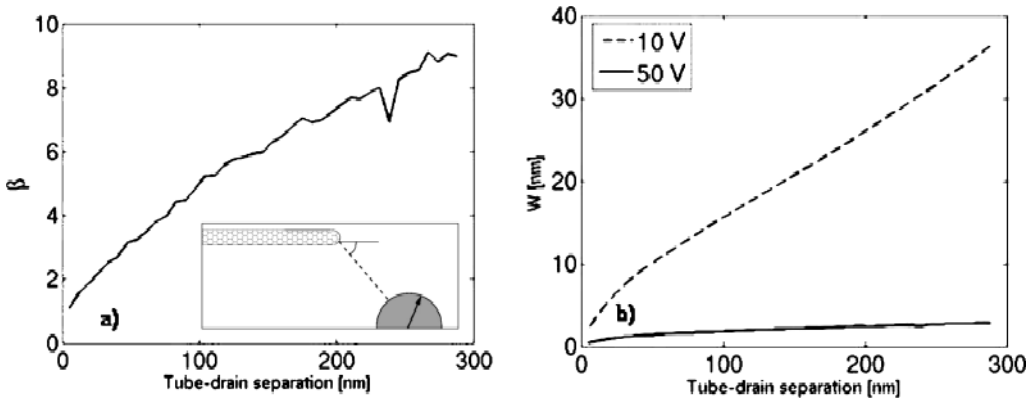

Figure 6. (a) Field enhancement factor β as a function of the nanotube–drain separation calculated for a 30 nm diameter nanotube. In this case, the field enhancement factor is a sub-linear function of the separation implying that the barrier width and emission current will depend on the separation. The inset shows the geometry used in the calculation. (b) Corresponding effective tunnel widths as a function of separation for two different values of the source–drain voltage (10 and 50 V). The effect is most pronounced for small source–drain voltages.

bends, changing $\bar{h}$, and consequently, the barrier width changes by

$$\delta W = \frac{\varphi}{V_{SD}} \frac{\beta\left(\bar{h}/d_o, b/d_o\right) - \left(\bar{h}/d_o\right)\beta'\left(\bar{h}/d_o, b/d_o\right)}{\beta^2\left(\bar{h}/d_o, b/d_o\right)} \frac{\partial \bar{h}}{\partial V_{SG}} \delta V_{SG}, \tag{2}$$

where $\beta'\left(\bar{h}/d_o, b/d_o\right)$ indicates the derivative with respect to the first argument. Hence, any nonlinearity in the field enhancement factor as a function of nanotube–drain separation results in a gate voltage-dependent barrier width and, consequently, a gate voltage-dependent source–drain impedance. Since the current is an exponential function of W, as shown by the Fowler–Nordheim relation

$$I \propto F^2 \exp\left(-\frac{W}{\lambda}\right), \tag{3}$$

where $\lambda(\varphi)$ is the tunnelling length, even a small nonlinearity may have a large effect. If, however, the local field varies appreciably within distance W from the nanotube tip, the argument of the exponential above is changed to $-W(\varphi)/\lambda(\varphi)$, where $W(\varphi)$ is the distance from the nanotube when the electrostatic potential has increased by φ/e. In many cases, the simple discussion in terms of β is sufficient for field emission from nanotubes at source–drain voltages exceeding approximately 50 V, whereas transport at lower voltages requires a more complete discussion.

Figure 6(a) depicts the field enhancement factor and figure 6(b) the effective barrier widths (assuming a work function of 4 eV (Semet *et al* 2002) and applied voltages of 10 and 50 V) for a number of nanorelay structures comprising a 30 nm diameter carbon nanotube and a semi-cylindrical drain electrode at a varying distance from the nanotube tip. As shown in figure 6(a), the field enhancement in this geometry is a sub-linear function of the nanotube–drain separation, implying that the barrier width and the emission current depend on the distance. The dependence

is more pronounced at small source–drain voltages when the barrier width is almost a linear function of the nanotube–drain separation, as shown in figure 6(b). In the far-drain structures with large field enhancement at the nanotube tip, electrons are more easily extracted from the nanotube than from the drain, rendering the I_D–V_{SD} characteristics asymmetric in agreement with other field-emission-based devices.

3. Fabrication of nanorelay devices

The multiwalled nanotubes used for fabricating the nanorelay devices were synthesized by plasma-enhanced chemical vapour deposition (Morjan *et al* 2004, Yao *et al* 2005). They are not perfect hollow structures with concentric defect-free graphitic cylinders but typically have a bamboo-like geometry for diameters less than about 50 nm and should be more correctly regarded as nanofibres for larger diameters where the walls are formed of graphitic planes in a herring-bone geometry (Yao *et al* 2005). The work function for such nanotubes/nanofibres is approximately 4 eV (Semet *et al* 2002) and the Young's modulus is typically a few hundred GPa. The length of the nanotubes was typically 2–3 μm and the diameters of the nanotubes used for fabrication spanned the range 5–100 nm with the majority of tested structures having diameters of 20–50 nm.

The method used for fabricating the suspended nanotubes has been described previously (Lee *et al* 2004a, b). Gold electrodes are patterned on a silicon chip with the source electrodes considerably higher (typically by 135–200 nm) than the gate and drain electrodes. PMMA is then spin-coated on top of the gate and drain electrodes and oxygen plasma ashed to be the same height as the source electrode. This provides a support for the deposited nanotubes which are aligned and positioned using the ac-dielectrophoresis technique. After deposition, a top electrode (5 nm Ti, 70 nm Au) is placed over the nanotube at the source to ensure good contact, involving an additional lithography step. The PMMA is then carefully removed to produce a nanotube suspended over the gate and drain electrodes. Figure 7(a) shows a picture of the patterned chip after deposition of the nanotubes. Most source electrodes have captured one or two nanotubes. A typical contact-mode device is shown in figure 7(b). In the first experiments, it was found that mainly thick and long nanotubes remained suspended after processing. The statistics from one chip are shown in figure 8(a). This situation was greatly improved by introducing critical point drying for removal of the PMMA. The statistics from a chip prepared in this way are shown in figure 8(b) and it is clear that this improvement allows the suspension of much thinner nanotubes with a large range of lengths L. An example of such a device is shown on figure 7(c).

One disadvantage of the fabrication method is that it does not provide good control over the length of the nanotube protruding from the source electrode (L). Not all suspended devices are suitable for nanorelay operation because of this. Devices with L comparable to the distance between the source and drain electrode are suitable for testing the contact-mode operation while those with L slightly shorter than this, figure 7(d), can be used for testing the non-contact mode. An additional problem is that many nanotubes are not suspended horizontally but are suspended at an angle towards the substrate making it difficult to be certain about the initial vertical distance between the nanotube and the gate and drain electrodes. These complications mean that the operating characteristics of each device are slightly different.

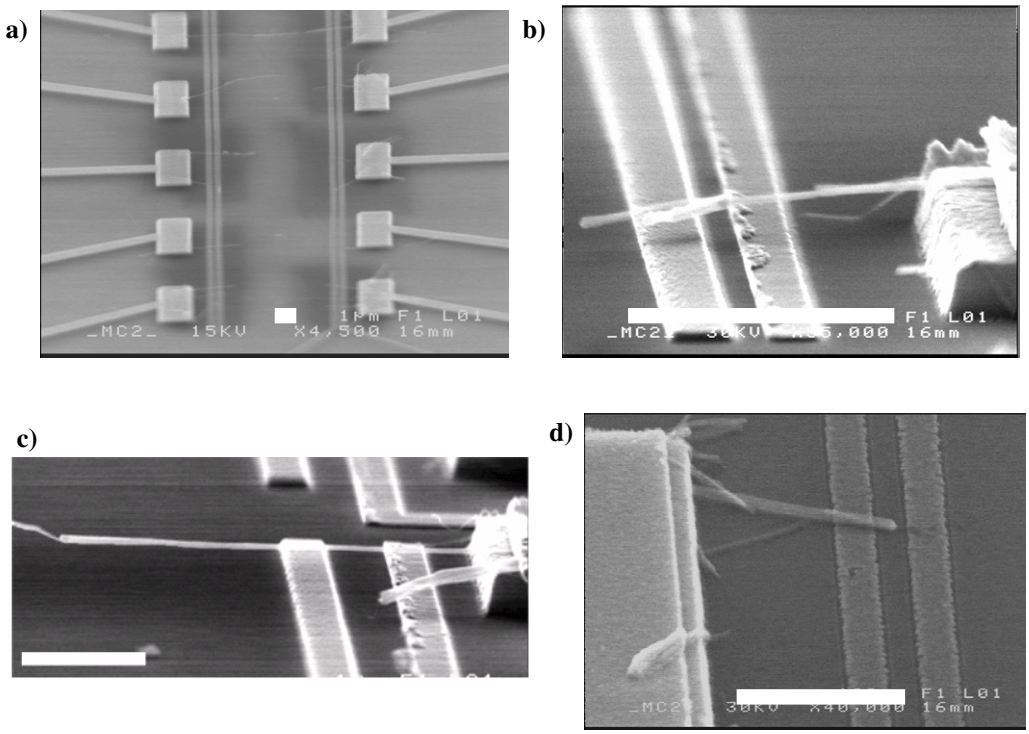

Figure 7. SEM pictures of relay structures. The white bar represents a length of 1 μm. (a) An overview of chip pattern, (b) contact mode relay, (c) very long thin nanotube suspended after introducing the critical point drying technique and (d) non-contact mode relay.

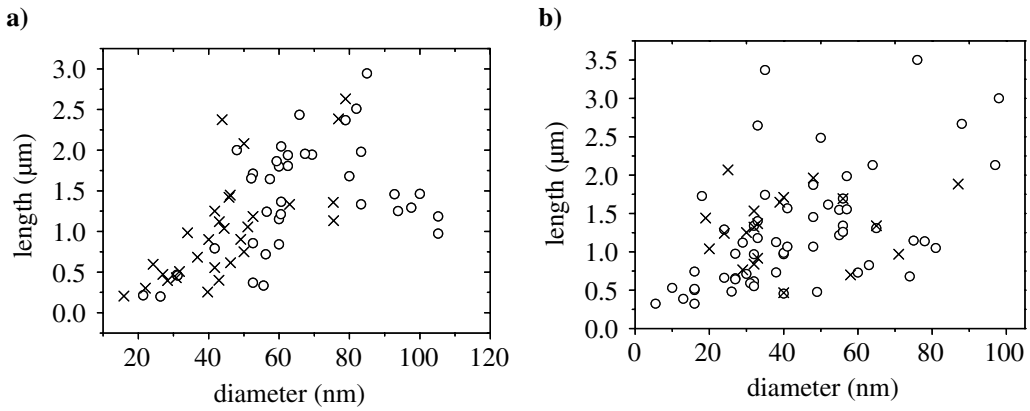

Figure 8. Statistics of the success rate in producing suspended nanotubes from two different chips. Circles indicate that the structure was successfully suspended, crosses indicate that it had contact with the substrate. (a) A chip prepared without using critical point drying in the final stage. Note that thin nanotubes (<50 nm diameter) are mainly not suspended. (b) A chip prepared by using critical point drying. A much higher success rate is obtained for the thin and short nanotubes.

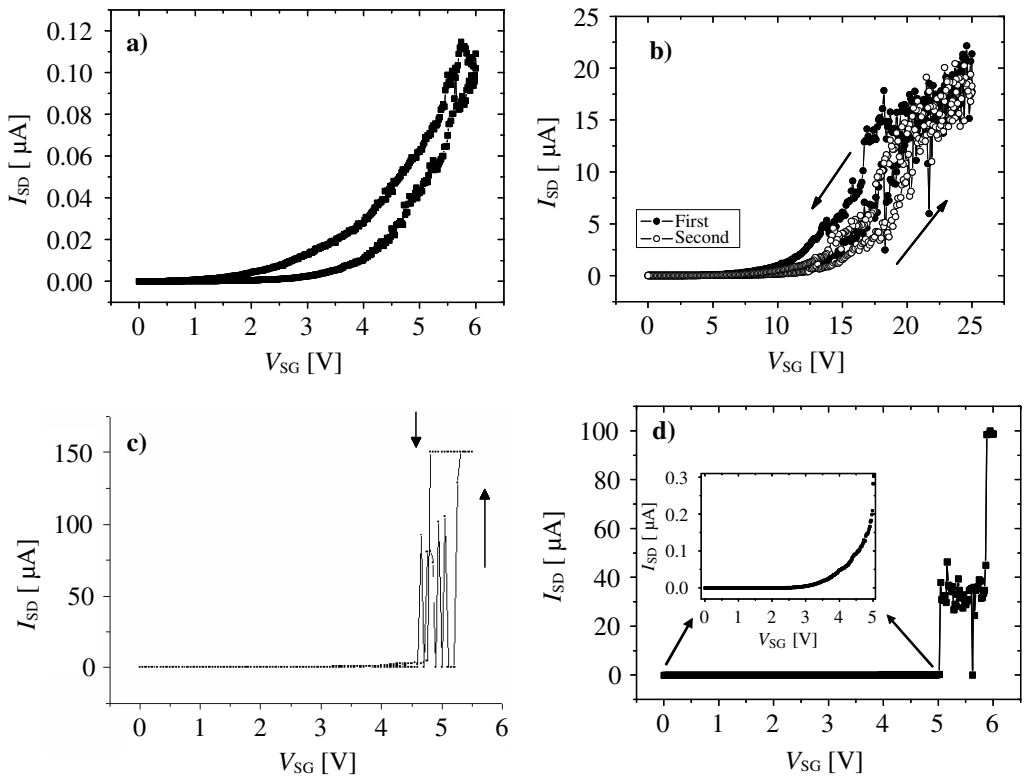

Figure 9. Results of relay measurements on four different contact mode devices with a source–drain bias of 0.5 V. (a), (b) The expected hysteresis but with a slower turn-on than expected. (c) The sharp turn-on and turn-off predicted theoretically. Note that this was a two terminal device (i.e. the gate and drain electrodes were electrically connected). (d) Illustration of the 'stiction' problem. This nanotube made contact with the drain electrode at a gate voltage of 5 V and the gate electrode at 6 V. It stuck to the electrodes and it was not possible to remove it when the gate voltage was reduced to zero.

4. Experimental characterization and comparison with theoretical models

4.1. Contact-mode

Figure 9 shows some typical I_D–V_{SG} characteristics of contact-mode relays where the nanotube is long enough to make physical contact with the drain electrode. All measurements were carried out in air at room temperature with a source–drain bias voltage of 0.5 V. Figures 9(a) and (b) show the results of nanorelays where the nanotube did not stick to the drain electrode on contact. In this case, one observes a relatively slow onset of the source–drain current with increasing gate voltage and a clear hysteresis effect. Multiple cycles are possible. In figure 9(b) the source–drain current is very high (20 μA) leading to significant heating of the nanotube. This affects the I_D–V_{SG} characteristics leading to a slight decrease in the current on the second scan for the same gate voltage values and a slight decrease in the hysteresis (higher turn-off gate voltage). Since the measurements are performed under atmospheric conditions, the I_D–V_{SG} characteristics are likely to be strongly influenced by the presence of adsorbates, in particular water. At present,

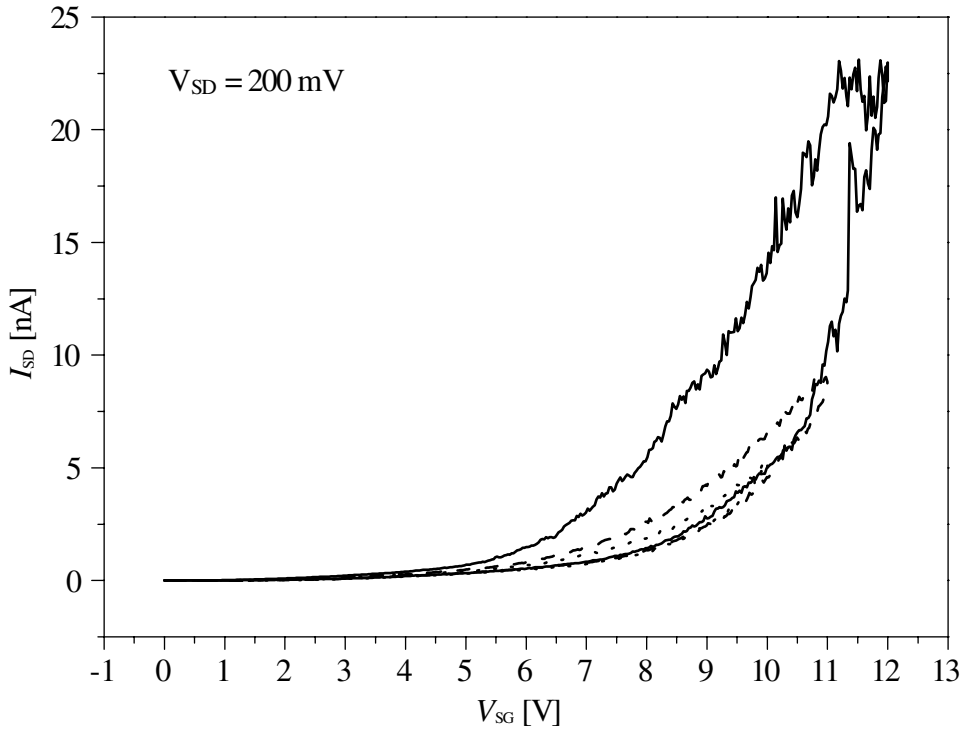

Figure 10. I_{SD} versus V_{SG} for a contact-mode device. The results of three gate voltages scans are shown. On each scan the maximum gate voltage is increased. Scan 1 (· · · · · ·): $V_{SG}(\text{max}) = 10\,\text{V}$. Scan 2 (- - - -) $V_{SG}(\text{max}) = 11\,\text{V}$. Scan 3 (——) $V_{SG}(\text{max}) = 12\,\text{V}$. The amount of hysteresis increases as the maximum gate voltage increases, corresponding to stronger interaction between the nanotube and the drain.

we believe that the slow current turn-on and lack of 'stiction' in these devices may be due to tunnelling through layers of adsorbates on both the nanotube and the drain electrode surfaces; however, this remains to be studied systematically. In these devices, we have probably not applied a large enough gate voltage to make direct physical contact between the nanotube and the drain. Some evidence for this can be seen in figure 10. Here, we show multiple scans on a single relay device where the maximum gate voltage has been increased on each scan. The current through the device is relatively low (20 nA) and we do not expect strong heating effects in this case. It is clear from this plot that the extent of the hysteresis increases as the maximum gate voltage increases, i.e. as the nanotube is moved closer to the drain electrode.

The results shown in figures 9(c) and (d) are more similar to the theoretical predictions in terms of the abruptness of the current switching. In the case of figure 9(c), the gate and drain electrodes were connected so that it is more correctly regarded as a two-terminal relay. The much higher currents observed ($>150\,\mu$A) can be partially attributed to the higher source–drain voltage (in this case equal to the source–gate voltage). Here, we observe strong fluctuations in the current as contact is made with the drain. On physical contact at $V_G = 5.3\,\text{V}$, the current increases sharply beyond the compliance value of the current set on the measuring instrument ($150\,\mu$A). One then observes the expected hysteresis and a sharp turn-off behaviour at a gate voltage of 4.7 V. Hysteresis was also observed on the second gate voltage scan with this device

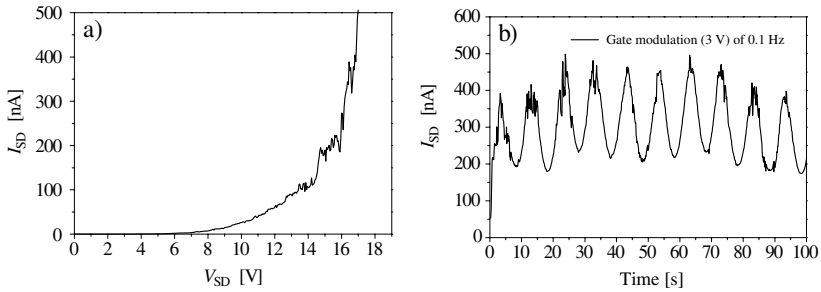

Figure 11. (a) Source–drain current versus source–drain voltage for a non-contact mode nanorelay device (no gate voltage applied). (b) Modulation of the source–drain current from the same device by applying an oscillating gate voltage. The current modulation is in phase with the voltage applied to the gate electrode.

but the current levels reached were much lower than on the first scan. This may be partially a consequence of adsorbate removal due to the high temperatures produced on the first scan but is probably mainly due to the burning-off of the outer nanotube walls, as has been observed in SEM pictures taken after device testing. This may also be the reason why the nanotube was released from the substrate on the first scan. In figure 9(d), the nanotube has made physical contact first with the drain electrode, at $V_G = 5$ V and then with the gate electrode when the voltage is increased to $V_G = 6$ V. Note that the behaviour before the sharp current increase is similar to that shown on figures 9(a) and (b), as is the case also for figure 9(c). For the device shown in figure 9(d), the nanotube remained fixed to the gate and drain electrodes as the gate voltage was reduced to zero.

The gate voltages required to make electrical contact between the nanotube and the drain are very close to those predicted theoretically. This may be somewhat surprising considering that the dimensions of the experimental devices are considerably larger than those used for the original contact-mode model (see section 2). However, fortunately the effects of the larger dimensions used experimentally cancel each other out to a large extent. The larger height, h, and nanotube diameter, d_o, are compensated for by the greater length, L, and poorer Young's modulus of the nanotubes used in the experiments. The hysteretic behaviour predicted theoretically has been observed; however, the onset is more gradual with increasing gate voltage in the experiments which we can attribute to the effect of adsorbate layers on both the nanotube and the electrode surfaces.

4.2. Non-contact mode

Figure 11 shows measurements made on a non-contact device where the nanotube is not long enough to make physical contact with the drain. These measurements were carried out under high vacuum conditions (10^{-6} mbar). Figure 11(a) shows the dependence of the source–drain current on the source–drain voltage for zero gate voltage. The original distance of the nanotube tip from the electrode surface was nominally 180 nm, however this is very difficult to determine experimentally and it may be slightly less than this due to an initial misalignment of the nanotube from the horizontal configuration. The field emission current onsets at a source–drain voltage of about 8 V and then increases nonlinearly as the source–drain voltage, and hence applied electric field, is further increased. The high source–drain voltage may also serve to deflect the

nanotube so that the nanotube–drain distance may decrease for high-applied fields. This will further enhance the field emission current according to the calculations shown in figure 6, since in the distance range of interest the field enhancement factor, β, increases less than linearly with the separation.

The effect of applying a gate voltage is shown in figure 11(b) for a fixed value of the source–drain voltage (10 V). The current increases from about 50 to 400 nA on the first increase of the gate voltage. There is then a clear and reproducible modulation of the current with the gate voltage, in phase with the gate voltage, although the current never decreases to the starting value, indicating that an irreversible change in the nanorelay geometry has occurred on the first increase in gate voltage. If one considers the field enhancement calculations discussed in section 2, one can estimate that the observed modulation in the field emission current could be expected for a small change in the nanotube tip–drain electrode distance. If the initial distance is taken to be 180 nm, then the measured modulation could be achieved if the gate voltage served to reduce that distance by approximately 25 nm. Although the applied voltage is rather small, this appears to be feasible in light of the measurements on the contact-mode structures. Of course, this is greatly simplifying the situation and other effects will need to be taken into consideration such as the effect of the potential changes on the large gate electrode on the local field at the nanotube tip even in the case of zero deflection. Numerical evaluation of this effect suggests that it could result in local field changes of a few per cent, similar in magnitude to the effects of a deflection on the order of 25 nm.

More detailed experimental results are needed to better test the theoretical model of the non-contact mode nanorelay. One major question concerns the magnitude of the field emission current. The theoretical calculations predict that the emission current should be negligible for an applied source–drain voltage of 10 V and the experimental geometry. There are a number of reasons why the experimental field emission current may be larger than the theoretically predicted one. The calculations assume a work function of 4 eV. This has been determined for vertically aligned arrays of similar plasma-CVD grown nanotubes/nanofibres (Semet *et al* 2002). These measurements were carried out after conditioning to remove all effects of adsorbate species. In our experiments, we do not specifically remove the adsorbates and, as we have seen from the contact-mode measurements, this can strongly influence the experimental results. It has been shown that the presence of adsorbates, particularly water, can increase the emission current by orders of magnitude (Dean *et al* 1999). This can be due to a significant decrease of the work function (Maiti *et al* 2002) and/or can be a consequence of adsorbate resonant tunnelling states (Dean *et al* 1999). An additional effect could be due to the geometry of the nanotube. As stated previously, the Ni-catalysed plasma-CVD grown nanotube/nanofibres do not have perfect multiwalled nanotube structures. They may also have Ni particles at the tip (as is the case for the non-contact mode structure shown in figure 7(d)). The arrangement of the graphitic planes at the tip of the structure, combined with structural defects may well lead to larger local fields than have been considered so far.

5. Conclusion

We have considered a theoretical model of a three-terminal carbon nanotube nanorelay. The device is based on a nanotube fixed at one end to a source electrode and freely suspended over a gate and drain electrode. The nanorelay is considered to operate in two different modes, referred

to as the contact and non-contact modes. The contact mode operates with low source–drain voltages. The relay is switched to the on state by applying a gate voltage that serves to deflect the suspended nanotube until it makes contact with the drain. The non-contact mode operates at higher source–drain voltages (higher than the nanotube work function) and relies on electron field emission between the nanotube and drain electrode for electrical contact. The magnitude of the field emission is controlled by applying a gate voltage to modulate the nanotube–drain distance. The theoretical predictions have been compared with measurements on nanorelays prepared by depositing nanotubes on patterned substrates, making use of a PMMA support which can then be removed using critical point drying, to produce the suspended nanotube. Both contact and non-contact mode structures have been prepared and tested. The contact mode structures show behaviour similar to the theoretical predictions. The problem of 'stiction' is alleviated by a layer of adsorbates, allowing working nanorelays to be demonstrated. First measurements on non-contact mode devices show that it is possible to use field emission to make electrical contact between the source and drain and that the field emission current can be modulated by applying a gate voltage. More work is needed to quantify the behaviour of the relays and to obtain more information concerning the influence of adsorbates on the operating characteristics.

It would be of interest to test nanorelays with better quality multiwalled nanotubes and to carry out systematic measurements relating to the adsorbate question. The experiments are very challenging and time consuming due to the lack of control over the precise dimensions, in particular the length of the nanotube extending from the source (L) and the initial height (h) of the nanorelay above the gate and drain electrodes. Attempts are underway to develop a method of directly growing nanorelays in a vertical configuration that should hopefully lead to more reproducible and reliable experimental conditions.

Acknowledgments

Financial support from STINT (Stiftelsen för internationalisering av högre utbildning och forskning), SSF through the carbon-based NEMS framework programme and the EC (contract number FP6-2004-IST-003673, CANEL) is gratefully acknowledged. This publication reflects the views of the authors and not necessarily those of the EC. The Community is not liable for any use that may be made of the information contained herein. The Korean co-authors were also supported by the NSI-NCRC program of the KOSEF, MOST and the BK21 of MOE, Korea. YWP is grateful to the Royal Swedish Academy of Sciences (KVA) for partially supporting his stay in Sweden.

References

Axelsson S 2004 *MSC Thesis* Chalmers University of Technology, Gothenburg

Collins P G, Hersam M, Arnold M, Martel R and Avouris Ph 2001 *Phys. Rev. Lett.* **86** 3128

Dean K A, von Allmen P and Chalamala B R 1999 *J. Vac. Sci. Technol.* **17** 1959

Desquesnes M, Rotkin S V and Aluru N R 2002 *Nanotechnology* **13** 120

Dresselhaus M S, Dresselhaus G and Avouris Ph (ed) 2001 *Carbon Nanotubes, Synthesis, Structure, Properties and Applications* (Heidelberg: Springer)

Hwang H J and Kang J W 2005 *Physica* E **27** 163

Ingold G L and Nazarov Y V 1992 *Single Charge Tunneling: Proc. NATO ASI* vol 294, ed M H Devoret and H Grabert (New York: Plenum) p 21

Jonsson L M, Nord T, Kinaret J and Viefers S 2004a *J. Appl. Phys.* **96** 629
Jonsson L M, Axelsson S, Nord T, Viefers S and Kinaret J 2004b *Nanotechnology* **15** 1497
Ke C and Espinosa H D 2004 *Appl. Phys. Lett.* **85** 681
Kinaret J, Nord T and Viefers S 2003 *Appl. Phys. Lett.* **82** 1287
Lee S W, Lee D S, Morjan R E, Jhang S H, Sveningsson M, Nerushev O A, Park Y W and Campbell E E B 2004a *Nano Lett.* **4** 2027
Lee S W, Lee D S, Yu H Y, Campbell E E B and Park Y W 2004b *Appl. Phys.* A **78** 283
Maiti A, Andzelm J, Svizhenko A, Anantram M P and in hetPanhuis M 2002 *Phys. Status Solidi* b **233** 49
Morjan R E, Kabir M S, Lee S W, Nerushev O A, Lindgren P, Bengtsson S, Park Y W and Campbell E E B 2004 *Curr. Appl. Phys.* **4** 591
Semet V, Binh V T, Vincent P, Guillot D, Teo K B K, Chhowalla M, Amaratunga G A J, Milne W I, Legagneux P and Pribat D 2002 *Appl. Phys. Lett.* **81** 343
Sveningsson M, Podenok S, Hansen K, Svensson K, Olsson E and Campbell E E B 2005 in preparation
Yao Y M, Falk L K L, Morjan R E, Nerushev O A and Campbell E E B 2005 *J. Microsc.* **219** 69